Journal of Engineering Research

ISSN 2764-1317 vol. 6, n. 2, 2026

ARTICLE 11

Acceptance date: 06/04/2026

IMPLEMENTATION OF COMPUTATIONAL ROUTINES IN PYTHON FOR NUMERICAL ANALYSIS OF DISPLACEMENTS IN PLATES USING THE FINITE DIFFERENCE METHOD

Rafael Vinícius Martins Silva
ttp://lattes.cnpq.br/4553100695288044

Pedro Filipe De Luna Cunha

Vitória Régia Araújo Ribeiro
https://lattes.cnpq.br/6260684242816074

Yuri Sotero Bomfim Fraga
https://lattes.cnpq.br/5055016786232011

Jerfson Moura Lima
https://lattes.cnpq.br/4244744747948798

Gabriel Lima Oliveira Martins
https://lattes.cnpq.br/5748460529875608

Andre Augusto Nobrega Dantas
https://lattes.cnpq.br/3443223409799104

All content published in this journal is licensed under the Creative Commons Attribution 4.0 International License (CC BY 4.0).

Abstract: The structural analysis of plates is an important topic in civil engineering, as it allows us to understand how these structures deform and how internal stresses are distributed when subjected to different loads. However, in many cases, analytical solutions become complex or even unfeasible, especially when considering different geometries and boundary conditions. In this context, numerical methods become fundamental tools for solving these problems. This work presents the development and implementation of a computational routine for the analysis of displacements and bending moments in plates using the **Finite Difference Method (FDM).** The method basically consists of dividing the plate into a mesh of nodes and, based on this discretization, transforming the differential equations of the problem into a system of algebraic equations that can be solved numerically. From the displacements obtained, it is possible to calculate the bending moments in the principal directions of the plate. To verify the reliability of the developed algorithm, seven plate examples with different support conditions, dimensions, and loading types were analyzed. The numerical results were compared with analytical solutions available in the classical literature and with results obtained using structural analysis software. In general, good agreement was observed between the results, with relatively small errors that are acceptable for engineering applications. It was also observed that the accuracy of the results is directly related to the refinement of the mesh used: the smaller the discretization step, the greater the accuracy, although this implies longer processing time. Nevertheless, the algorithm demonstrated good performance and the ability to analyze different geometric configurations of plates. Thus, it is concluded that the developed computational routine proves to be an efficient tool for the numerical analysis of plates, contributing both to practical applications and to the learning and understanding of numerical methods applied to structural engineering.

Keywords: Finite Difference Method; plate analysis; numerical methods; structural analysis; displacements; bending moments.

INTRODUCTION

Structural analysis is a fundamental step in the design and sizing of structural systems, responsible for determining displacements, internal forces, and support reactions resulting from the action of external loads. With advances in construction techniques and the increasing complexity of modern structures, classical analytical methods become limited when applied to systems with a large number of elements and degrees of freedom. In this context, numerical methods have come to play a central role in contemporary structural engineering.

Framed structures (or skeletal structures) are composed of straight-axis members connected by structural nodes and can be analyzed from the perspective of continuous or discrete systems (ALVES FILHO, 2000). While continuous modeling ( ) considers an infinite number of differential elements and leads to exact analytical solutions, its practical application is limited in complex structural problems. On the other hand, the discrete approach allows the structure to be represented by a finite set of interconnected elements, resulting in approximate solutions with high computational efficiency (ALVES FILHO, 2000).

Among truss structures, planar and spatial trusses stand out. Planar trusses are two-dimensional structures composed of straight members connected by labeled nodes, in which loads act exclusively on the nodes and lie in the same plane as the structure. In their ideal form, the members are subjected only to axial tensile or compressive forces (KASSIMALI, 2011). Any loads applied along the members can be replaced by statically equivalent nodal forces (ALVES FILHO, 2000). This structural type is widely used in roof systems and bridges, as discussed by Hibbeler (2012).

Spatial trusses, in turn, have a three-dimensional configuration, consisting of members connected in such a way as to ensure spatial stability. Their fundamental geometric unit is the tetrahedron, composed of six members and four nodes (HIBBELER, 2012). This three-dimensional arrangement provides high structural stiffness with low self-weight, making it widely used in long-span structures.

The mathematical formulation of structural analysis must satisfy three fundamental relationships: the equilibrium equations, the constitutive relationships, and the compatibility conditions (MARTHA, 2010). The equilibrium equations ensure that the structure remains in global and local static equilibrium (ALVES FILHO, 2000). The constitutive relations describe the stress-strain behavior of the material, with Hooke's Law typically adopted for materials exhibiting linear-elastic behavior (KASSIMALI, 2011). Compatibility conditions, on the other hand, ensure geometric continuity between elements after deformation, preventing the occurrence of physical discontinuities (MARTHA, 2010).

In the field of numerical analysis, the Finite Element Method (FEM) has established itself as one of the primary computational tools for solving structural problems (HUTTON, 2003). The method is based on the discretization of the structure into interconnected finite elements, transforming the continuous problem into a matrix algebraic system. According to Belytschko and Fish (2007), the FEM involves fundamental stages of preprocessing, formulation of element equations, assembly of the global matrix, application of boundary conditions, and postprocessing of results.

For truss structures, the beam element constitutes the basic unit of discretization. The element stiffness matrix relates nodal forces and displacements, initially formulated in a local coordinate system (BELYTSCHKO; FISH, 2007). In two-dimensional and three-dimensional structures, it is necessary to transform this matrix to the global system using rotation matrices based on principal cosines (LOGAN, 2006; KASSIMALI, 2011). The universality of the stiffness matrix and the assembly procedure using the direct stiffness method reinforce the versatility of the FEM in complex structural problems (BELYTSCHKO; FISH, 2007).

Although commercial structural analysis software is widely available, the development of custom routines holds significant academic and technical relevance. The direct implementation of the Stiffness Method allows for a better understanding of the mathematical fundamentals involved, control over the assumptions adopted, and the possibility of future expansion to nonlinear analyses or more complex problems (LOGAN, 2006). Furthermore, the integration between geometric and structural mo-

deling in a CAD environment and numeric al analysis represents an important advance in the automation of the calculation process.

In this context, this work presents the development and implementation of a computational algorithm for the linear analysis of planar and spatial trusses using the Finite Element Method. The routine was developed in Python, utilizing libraries for matrix manipulation, graphical visualization, and reading files in DXF format, allowing for the direct import of structural models designed in a CAD environment. The implemented system automatically assembles the global stiffness matrix, applies the boundary conditions, and provides the nodal displacements in both numerical and graphical form.

The results obtained are validated by comparison with classic examples from the literature and with established structural analysis software, ensuring the consistency and reliability of the proposed methodology. The main contribution of this work lies in the development of an integrated computational tool that combines rigorous theoretical foundations, automated matrix implementation, and an accessible graphical interface, serving as a basis for future extensions involving nonlinear analyses and more complex structural applications.

METHODOLOGY

The methodology for solving the proposed problems followed a flowchart composed of nine main modules or core components, which served as the organizational structure. The planning and design of the flowchart enabled the implemented algorithm to possess characteristics of easy understanding and rapid configuration for subsequent plates, as shown in Figure 1. There were also minor reformulations of some steps to accommodate, for example, the variability of length and width dimensions, as well as some additional repetition loops for the purpose of constructing the matrix of variables.

After completing Module 3, we proceed to Module 4, which has a unique feature regarding the initial process of converting linear equations into a matrix format. A specific function from the *SymPy* library is used, which resulted in significant processing time when higher precision was required by reducing the value of the step size *h.*

The results are then presented. A map and a color bar were used to provide an easy-to-understand visualization. The algorithm displays the maximum and minimum values of the displacements and bending moments, which are located in *the z-component* of the coordinate matrix.

Calculation Methods – Analytical

To validate the presented results, the work of Stephen Timoshenko and S. Woinowsky-Krieger, authors of the book *Theory of Plates and Shells – 2nd Ed. – 1959,* was utilized. Below are some tables extracted from the aforementioned reference, based on the different configurations of the plate edge supports. The analytical results are derived from these tables by analyzing the *b/a* ratio.

Calculation Methods – MDF

The application of FEM in solving plate deflection problems begins with the discretization of the plate into elements called nodes. It becomes evident after solving the problem using FEM that the number

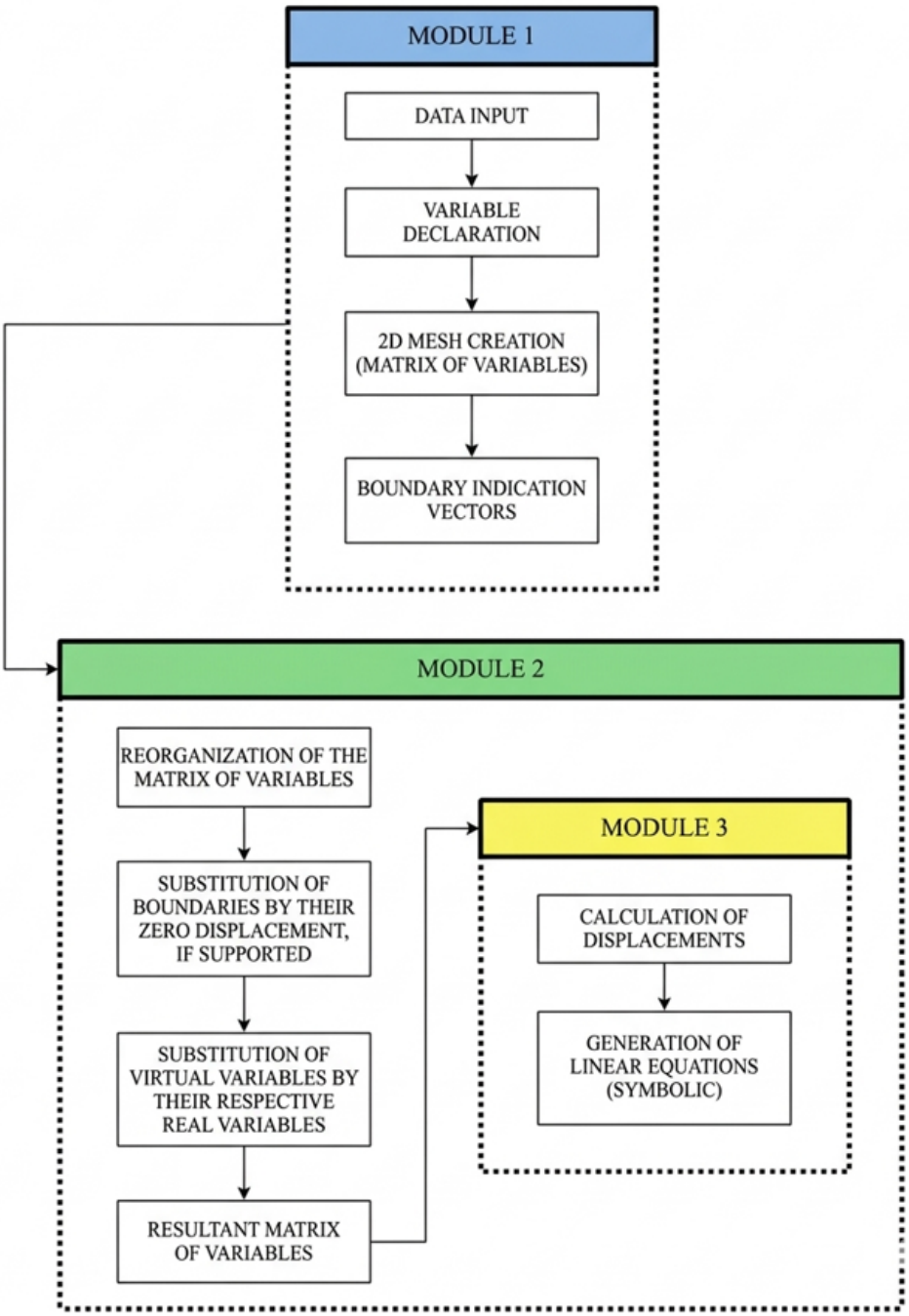


Figure 1 - General analysis method established - Part 1.

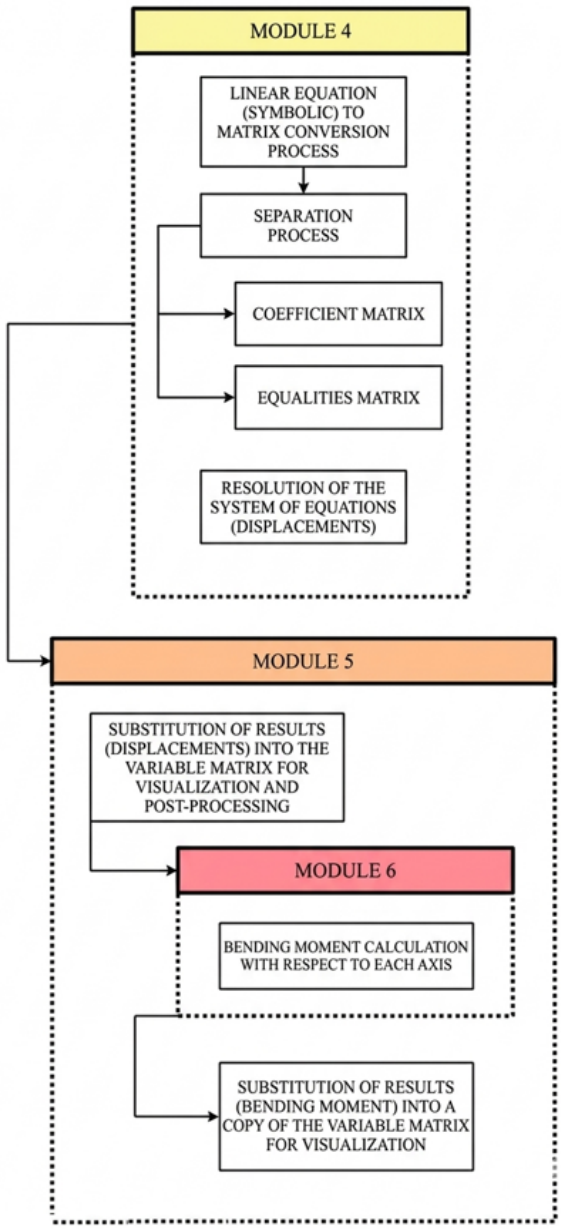


Figure 2 - General analysis method established - Part 2.

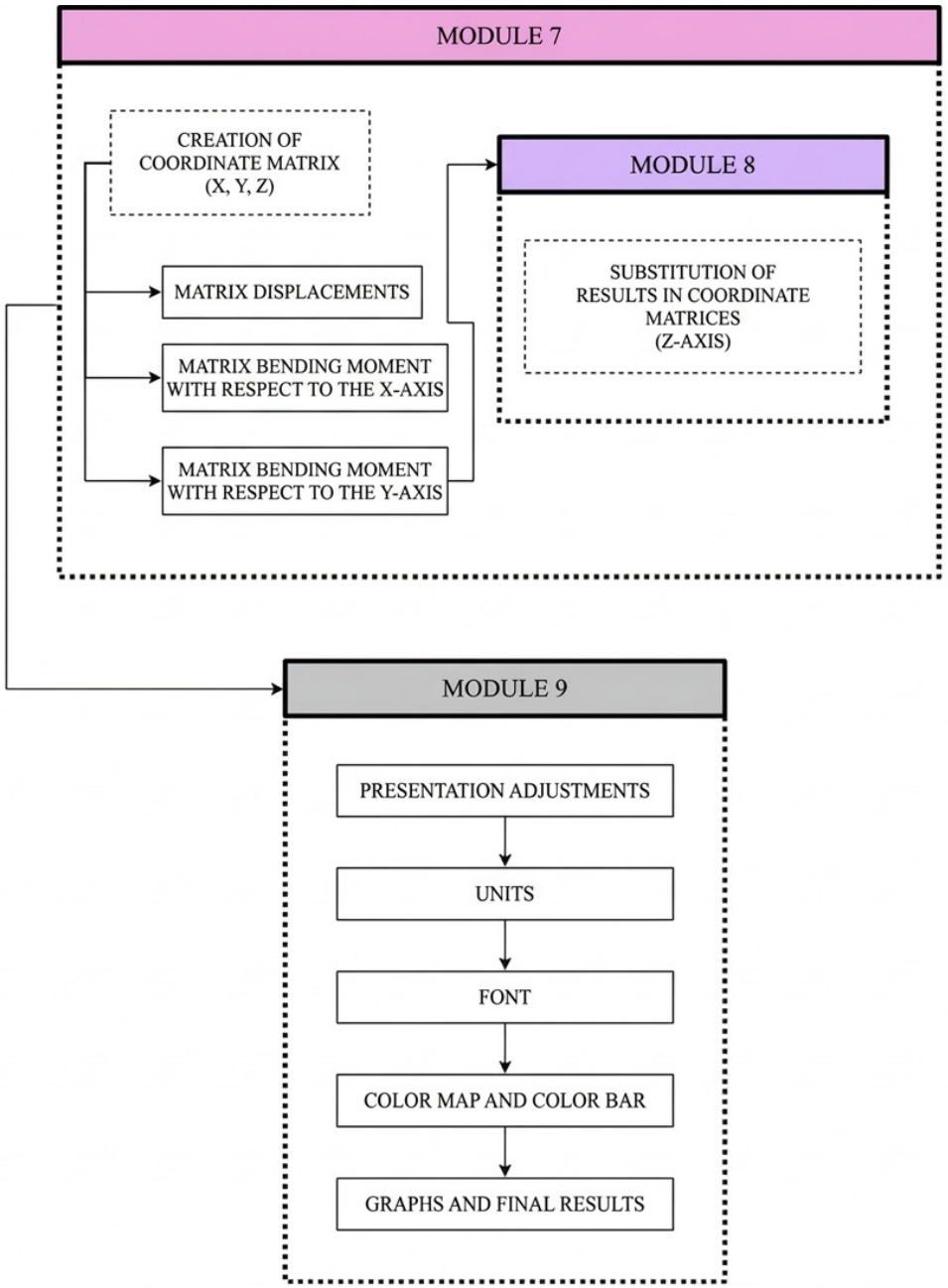


Figure 3 - General analysis method established - Part 3.

υ = 0.3					
b/a	$(w)_{x=0, y=0}$	$(M_x)_{x=a/2, y=0}$	$(M_y)_{x=0, y=b/2}$	$(M_x)_{x=0, y=0}$	$(M_y)_{x=0, y=0}$
1.0	$0.00126qa^4 / D$	$-0.0513qa^2$	$-0.0513qa^2$	$0.0231qa^2$	$0.0231qa^2$
1.1	$0.00150qa^4 / D$	$-0.0581qa^2$	$-0.0538qa^2$	$0.0264qa^2$	$0.0231qa^2$
1.2	$0.00172qa^4 / D$	$-0.0639qa^2$	$-0.0554qa^2$	$0.0299qa^2$	$0.0228qa^2$
1.3	$0.00191qa^4 / D$	$-0.0687qa^2$	$-0.0563qa^2$	$0.0327qa^2$	$0.0222qa^2$
1.4	$0.00207qa^4 / D$	$-0.0726qa^2$	$-0.0568qa^2$	$0.0349qa^2$	$0.0212qa^2$
1.5	$0.00220qa^4 / D$	$-0.0757qa^2$	$-0.0570qa^2$	$0.0368qa^2$	$0.0203qa^2$
1.6	$0.00230qa^4 / D$	$-0.078qa^2$	$-0.0571qa^2$	$0.0381qa^2$	$0.0193qa^2$
1.7	$0.00238qa^4 / D$	$-0.0799qa^2$	$-0.0571qa^2$	$0.0392qa^2$	$0.0182qa^2$
1.8	$0.00245qa^4 / D$	$-0.0812qa^2$	$-0.0571qa^2$	$0.0401qa^2$	$0.0174qa^2$
1.9	$0.00249qa^4 / D$	$-0.0822qa^2$	$-0.0571qa^2$	$0.0407qa^2$	$0.0165qa^2$
2.0	$0.00254qa^4 / D$	$-0.0829qa^2$	$-0.0571qa^2$	$0.0412qa^2$	$0.0158qa^2$
∞	$0.00260qa^4 / D$	$-0.0833qa^2$	$-0.0571qa^2$	$0.0417qa^2$	$0.0125qa^2$

Table 1 - Rectangular plates with fully fixed edges (Timoshenko and Woinowsky-Krieger, 1959).

	υ = 0.3							
b/a	$w_{max} = \alpha qa^4 / D$	$(M_x)_{max} = \beta qa^2$	$(M_y)_{max} = \beta_1 qa^2$	$(Q_x)_{(max)} = \gamma qa$	$(Q_y)_{max} = \gamma_1 qa$	$(V_x)_{max} = \delta_1 qa$	$(V_y)_{max} = \delta_1 qa$	$R = \eta qa^2$
	α	β	β_1	γ	γ_1	δ	δ_1	η
1.0	0.00406	0.0479	0.0479	0.338	0.388	0.420	0.420	0.065
1.1	0.00485	0.0554	0.0493	0.360	0.347	0.440	0.440	0.070
1.2	0.00564	0.0627	0.0501	0.380	0.353	0.455	0.453	0.074
1.3	0.00638	0.0694	0.0503	0.397	0.357	0.468	0.464	0.079
1.4	0.00705	0.0755	0.0502	0.411	0.361	0.478	0.471	0.083
1.5	0.00772	0.0812	0.0498	0.424	0.363	0.486	0.480	0.085
1.6	0.00830	0.0862	0.0492	0.435	0.365	0.491	0.485	0.086
1.7	0.00883	0.0908	0.0486	0.444	0.367	0.496	0.488	0.088
1.8	0.00931	0.0948	0.0479	0.452	0.368	0.499	0.491	0.090
1.9	0.00974	0.0985	0.0471	0.459	0.369	0.502	0.494	0.091
2.0	0.01013	0.1017	0.0464	0.465	0.370	0.503	0.496	0.092
3.0	0.01223	0.1189	0.0406	0.493	0.372	0.505	0.498	0.093
4.0	0.01282	0.1235	0.0384	0.498	0.372	0.502	0.500	0.094
5.0	0.01297	0.1246	0.0375	0.500	0.372	0.501	0.500	0.095
∞	0.01302	0.1250	0.0375	0.500	0.372	0.500	0.500	0.095

Table 2 - Rectangular plates with fully supported edges (Timoshenko and Woinowsky-Krieger, 1959).

DOI https://doi.org/10.22533/at.ed.13176226240211

υ = 0.3				
b/a	$(w)_{x=a/2, y=0}$	$(M_y)_{x=a/2, y=b/2}$	$(M_x)_{x=a/2, y=0}$	$(M_y)_{x=a/2, y=0}$
∞	$0.0130qa^4 / D$	$-0.125qa^2$	$0.125qa^2$	$0.037qa^2$
2.0	$0.0093qa^4 / D$	$-0.122qa^2$	$0.094qa^2$	$0.047qa^2$
1.5	$0.0064qa^4 / D$	$-0.112qa^2$	$0.069qa^2$	$0.048qa^2$
1.4	$0.0058qa^4 / D$	$-0.109qa^2$	$0.063qa^2$	0.047 square yards [2]
1.3	$0.0050qa^4 / D$	$-0.104qa^2$	$0.056qa^2$	$0.045qa^2$
1.2	$0.0043qa^4 / D$	$-0.098qa^2$	$0.049qa^2$	$0.044qa^2$
1.1	$0.0035qa^4 / D$	$-0.092qa^2$	$0.041qa^2$	$0.042qa^2$
1.0	$0.0028qa^4 / D$	$-0.084qa^2$	$0.034qa^2$	$0.039qa^2$
1/1.1	$0.0032qa^4 / D$	$-0.092qa^2$	$0.033qa^2$	$0.043qa^2$
1/1.2	$0.0035qa^4 / D$	$-0.098qa^2$	$0.032qa^2$	$0.047qa^2$
1/1.3	$0.0038qb^4 / D$	$-0.103qb^2$	$0.031qb^2$	$0.050qb^2$
1/1.4	$0.0040qb^4 / D$	$-0.108qb^2$	$0.030qb^2$	$0.052qb^2$
1/1.5	$0.0042qb^4 / D$	$-0.111qb^2$	$0.028qb^2$	$0.054qb^2$
0.5	$0.0049qb^4 / D$	$-0.122qb^2$	$0.023qb^2$	$0.060qb^2$
0.0	$0.0052qb^4 / D$	$-0.125qb^2$	$0.019qb^2$	$0.062qb^2$

Table 3 - Rectangular plates with one clamped edge and three supported edges (Timoshenko and Woinowsky-Krieger, 1959).

υ = 0.3				
b < a				
a/b	x=a/2, y=0 $w_{max} = \alpha\, qb^4 / D$ α	x=a/2, y=0 $M_x = \beta_1\, qb^2$ β_1	x = a/2, y = 0 $M_y = \beta_2\, qb^2$ β_2	x = a/2, y = b/2 $M_y = \gamma qb^2$ γ
∞	0.00260	0.0125	0.0417	-0.0833
2.0	0.00260	0.0142	0.0420	-0.0842
1.5	0.00247	0.0179	0.0406	-0.0822
1.4	0.00240	0.0192	0.0399	-0.0810
1.3	0.00234	0.0203	0.0388	-0.0794
1.2	0.00223	0.0215	0.0375	-0.0771
1.1	0.00209	0.0230	0.0355	-0.0739
b > a				
a/b	$w_{max} = \alpha\, qb^4 / D$ α	x=a/2, y=0 $M_x = \beta_1\, qa^2$ β_1	x=a/2, y=0 $M_y = \beta_2\, qa^2$ β_2	x=a/2, y=b/2 $M_y = \gamma qa^2$ γ
1	0.00192	0.0244	0.0332	-0.0697
1.1	0.00251	0.0307	0.0371	-0.0787
1.2	0.00319	0.0376	0.0400	-0.0868
1.3	0.00388	0.0446	0.0426	-0.0938

DOI https://doi.org/10.22533/at.ed.13176226240211

1.4	0.00460	0.0514	0.0448	-0.0998
1.5	0.00531	0.0585	0.0460	-0.1049
1.6	0.00603	0.0650	0.0469	-0.1090
1.7	0.00668	0.0712	0.0475	-0.1122
1.8	0.00732	0.0768	0.0477	-0.1152
1.9	0.00790	0.0821	0.0476	-0.1174
2.0	0.00844	0.0869	0.0474	-0.1191
3.0	0.01168	0.1144	0.0419	-0.1246
∞	0.01302	0.1250	0.0375	-0.1250

Table 4 - Rectangular plates with two clamped edges and two supported edges (Timoshenko and Woinowsky-Krieger, 1959).

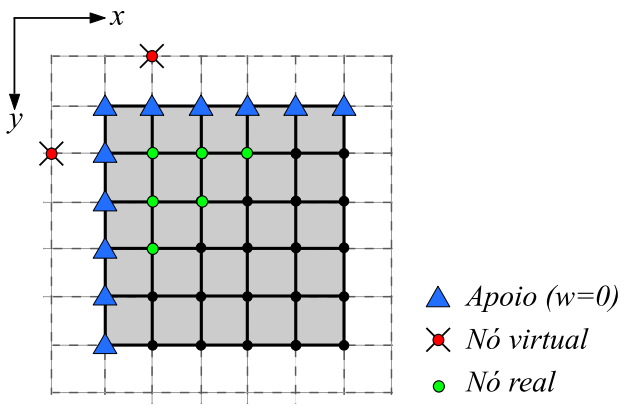


Figure 4 – Hypothetical plate and template cell for interior nodes.

of nodes chosen directly affects the results obtained. That is, a greater number of nodes reduces the error in the generated results, but increases computational cost.

After discretization, it is necessary to analyze the types of supports present in the plate under study. In general, the resulting template cell is used for interior nodes in the discretized mesh, causing it to traverse the entire mesh via loops, as shown in Figure 4.

It is important to note that virtual nodes must be created, which will compose the equations, thereby enabling their solution. Another important point is the orientation of the axes, which follows a location format as presented in the reference matrix in Figure 5. The origin of *the loops* is at the upper left position, serving as the basis for the virtual nodes.

$$\begin{bmatrix} w_{i,j} & \cdots & w_{i,j+n} \\ \vdots & \ddots & \vdots \\ w_{i+n,j} & \cdots & w_{i+n,j+n} \end{bmatrix}$$

Figure 5 – Reference matrix of node positions.

For a better understanding, here are two examples of pseudocode for calculating deflections and then bending moments (x or y), according to Figures 6 and 7.

Thus, a linear system of possible and determined equations is created. Using the obtained displacement results, the template cell is used to calculate the bending moments along the x and y axes.

AL RESULTS AND DISCUSSIONS

Seven examples were addressed, varying the loads, supports, and dimensions. The implemented routine calculates the deflection, the bending moment about the x-axis, and the bending moment about the y-axis. To validate the results, the tables from Section 2.1 were used.

Problem 1 – Fully pinned square plate

The following problem involves a fully clamped square plate with uniformly distributed loading, as shown in Figure 8. For this first problem, three values of the time step h were analyzed to demonstrate the elapsed times and the convergence of the displacements.

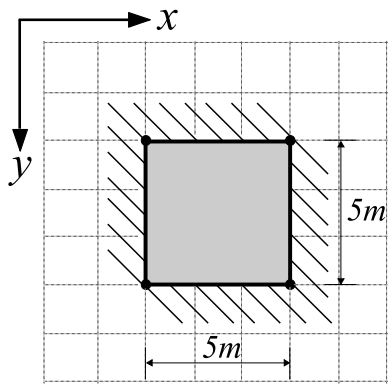


Figure 8 - Square plate with fully pinned edges.

For step size h = 0.50 m, the elapsed time was 4 seconds and the maximum displacement was 1.252 mm. Figures 9 and 10 show the displacement plots.

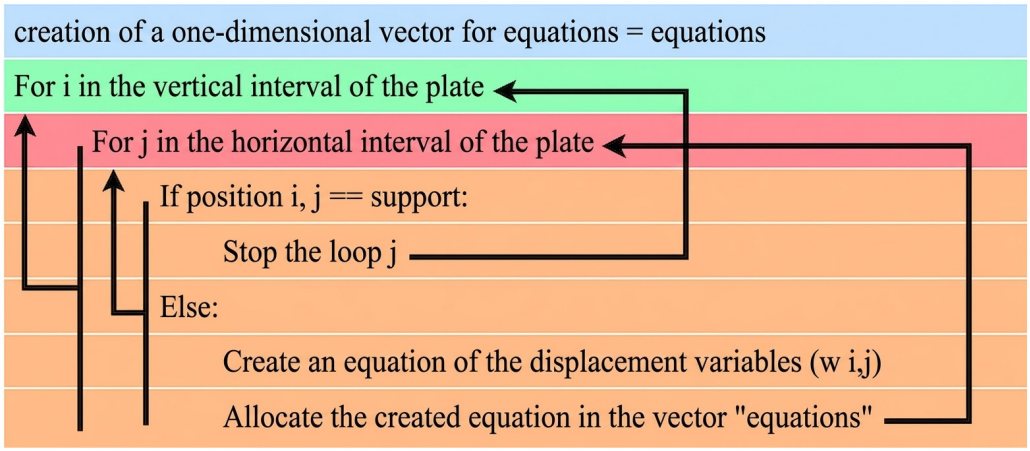


Figure 6 – Pseudocode for calculating deflections.

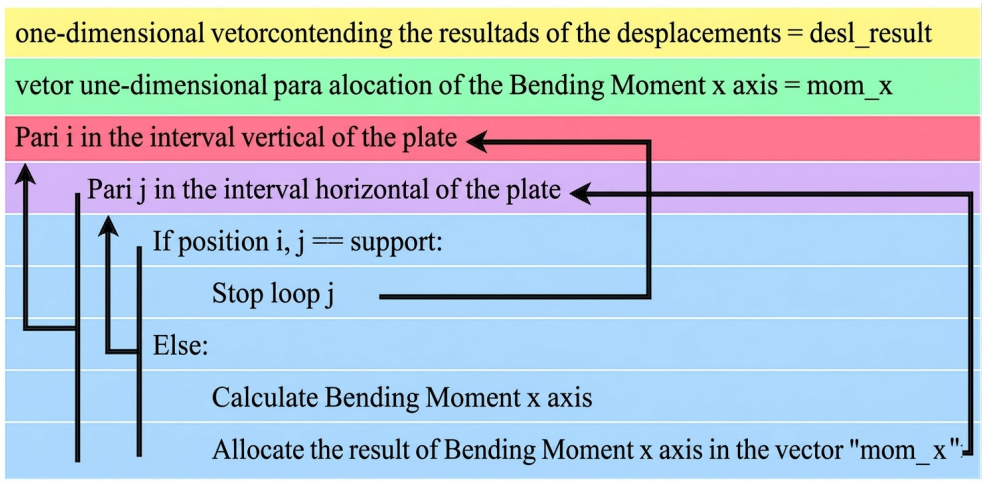


Figure 7 – Pseudocode for calculating bending moment x.

DOI https://doi.org/10.22533/at.ed.13176226240211

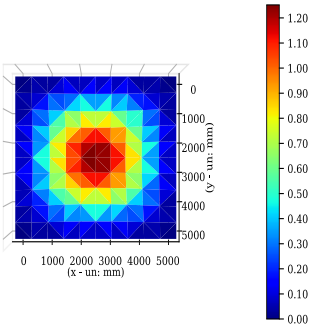


Figure 9 - Displacements (w) (h = 0.50 m) - View of the ***xy*** plane.

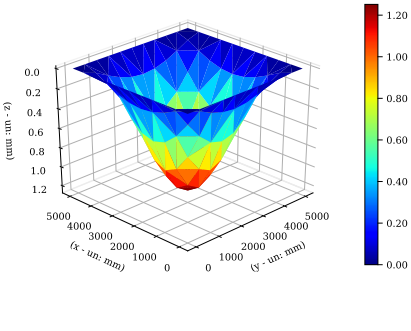


Figure 10 - Displacements (w) (h = 0.50 m) - 3D ***xyz*** view.

For a pitch of h = 0.25 m, the elapsed time was 31 seconds and the maximum displacement was 1.181 mm. Figures 11 and 12 show the displacement graphs.

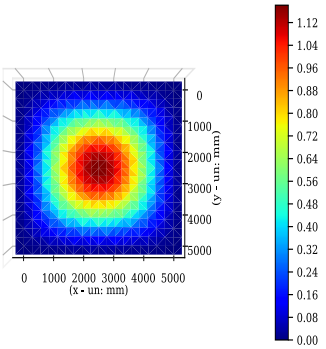


Figure 11 - Displacements (w) (h = 0.25 m) - View of the ***xy*** plane.

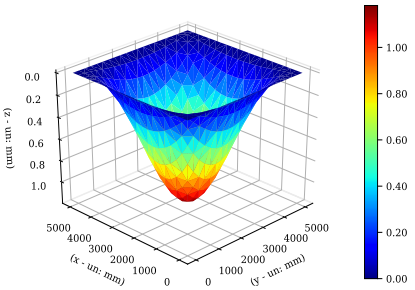


Figure 12 - Displacements (w) (h = 0.25 m) – 3D ***xyz*** view.

The initial assumptions adopted for the calculation for h = 0.125 m are presented in the following table.

The following are the results obtained for Problem 1 for mesh size h = 0.125 m:

The elapsed time was 8 minutes and 57 seconds. See section 2.6 for details on the machine used. In this first example, the algorithm produced satisfactory results and a reasonable execution time for the step size h = 0.125 m. A considerable increase in time is observed starting from the last step size

q	L	C	E	esp	υ	h
30 kN/m	5 m	5 m	$28x10^6$ kPa	20 cm	0.3	0.125 m
$D = \frac{Eesp^3}{12(1-\upsilon^2)} = 20512{,}82051\ KN.m$						

where:

Load = q;

Width = L;

Length = C;

Young's modulus = E;

Plate thickness = esp;

Poisson's ratio = υ

Mesh size = h;

Bending stiffness = D.

Table 5 – Assumptions adopted.

Results	$w_{máx}$ ((mm)	$M_{xmáx}$ (kN·m)	$M_{ymáx}$ (kN·m)
Algorithm	1.163	-38,387	-38.387
Analytical[1]	1,152	-38,475	-38,475
Error (%)	0.95	0.23	0.23

Table 6 – Results with step size h = 0.125 m.

1. The analytical solution is obtained from Table 1 for the ratio *b/a* = 1.

value adopted, due to the high number of 1,600 nodes. For the step sizes h = 0.50 m, there are 100 nodes, and for h = 0.25 m, there are 400 nodes. Figures 13, 14, 15, 16, 17, and 18 show the displacements and stresses in the plate under study.

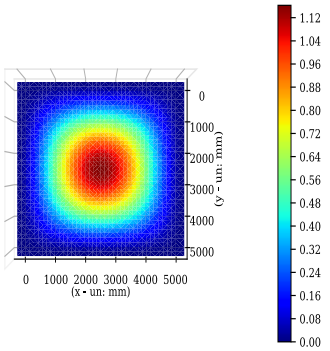


Figure 13 - Displacements (w) - View in the ***xy*** plane.

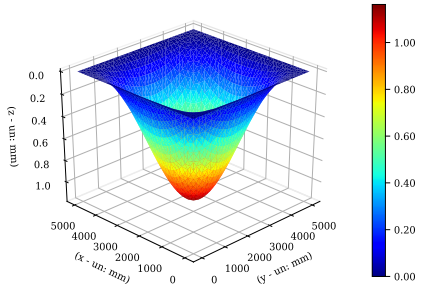


Figure 14 – Displacements (w) – 3D ***xyz*** view.

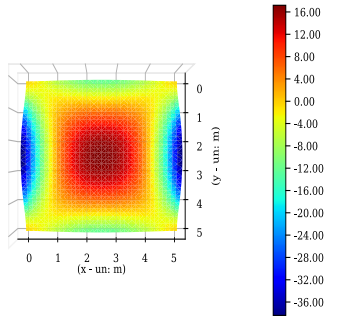


Figure 15 – Bending moment ***about the x-axis*** (M_x) – ***xy*** plane view.

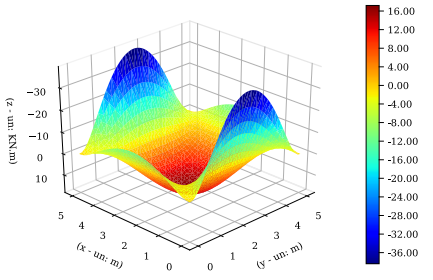


Figure 16 – Bending moment ***about the x-axis*** (M_x) – 3D ***xyz*** view.

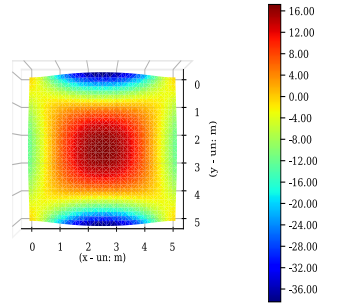


Figure 17 – Bending moment ***about the y-axis*** (M_y) – View in the ***xy*** plane.

DOI https://doi.org/10.22533/at.ed.13176226240211

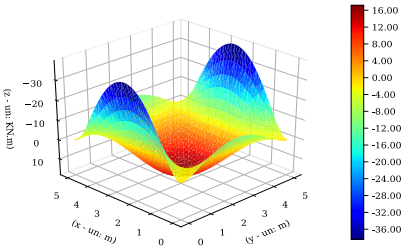


Figure 18 - Bending moment ***about the y-axis*** (M_y) - 3D ***xyz*** view.

Problem 2 – Fully supported square plate

The following problem involves a fully supported square plate with uniformly distributed loading, as shown in Figure 19.

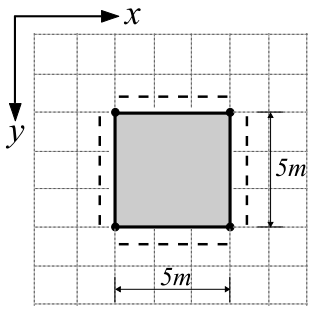


Figure 19 – Square plate with fully supported edges.

The initial considerations are shown in Table 7.

The following shows the results obtained for Problem 2:

The elapsed time was 12 minutes and 55 seconds. In this example, the results showed highly reduced errors and a slightly longer time compared to the previous example, thus demonstrating noticeable success in completing this example. Figures 20, 21, 22, 23, 24, and 25, in turn, represent the displacements and stress in the plate under study.

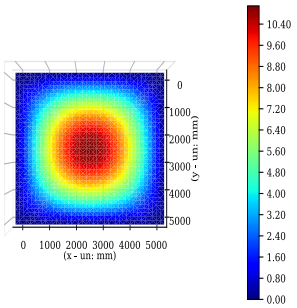


Figure 20 - Displacements (w) - View of the ***xy*** plane.

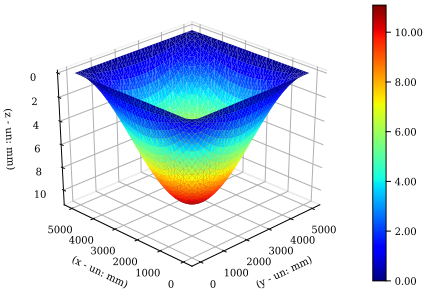


Figure 21 - Displacements (w) - 3D ***xyz*** view.

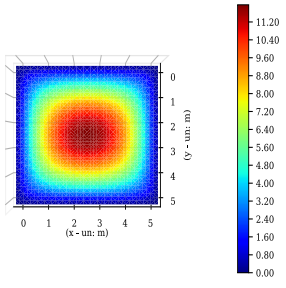


Figure 22 - Bending moment on ***the x-axis*** (M_x) - View in the ***xy*** plane.

q	L	C	E	esp	υ	h
10 kN/m	5 m	5 m	$25x10^6$ kPa	10 cm	0.3	0.125 m
$D = \frac{Eesp^3}{12(1-\upsilon^2)} = 2289{,}3773\ KN.m$						

Table 7 – Initial assumptions adopted.

Results	$w_{máx}$ (mm)	$M_{xmáx}$ (kN·m)	$M_{ymáx}$ (kN·m)
Algorithm	11.089	11.966	11,966
Analytical[1]	11,086	11,975	11,975
Error (%)	0.03	0.08	0.08

Table 8—Results obtained.

q	L	C	E	esp	υ	h
10 kN/m	5 m	5 m	$25x10^6$ kPa	10 cm	0.3	0.125 m
$D = \frac{Eesp^3}{12(1-\upsilon^2)} = 2289{,}3773\ KN.m$						

Table 9 – Initial assumptions adopted.

Results	$w_{máx}$ (mm)	$M_{xmáx}$ (kN·m)	$M_{ymáx}$ (kN·m)
Algorithm	7.806	-20.902	8.796
Analytical[2]	7,644	-21,000	8,500
Error (%)	2.12	0.47	3.48

Table 10—Results obtained.

1. The analytical solution is obtained from Table 2 for the ratio *b*/*a* = 1.
2. The analytical solution is obtained from Table 3 for the ratio *b*/*a* = 1.

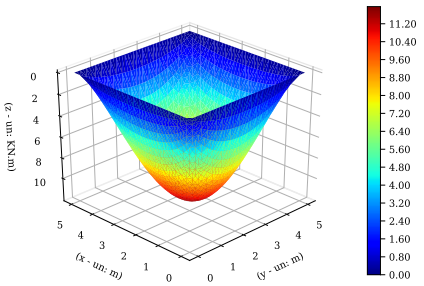


Figure 23 - Bending moment ***about the x-axis*** (M_x) - 3D ***xyz*** view.

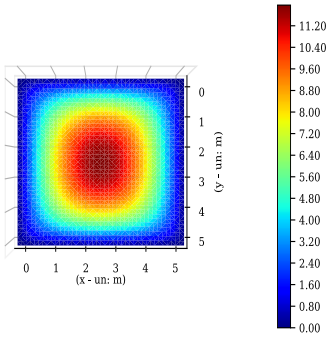


Figure 24 - Bending moment ***about the y-axis*** (M_y) - View in the ***xy*** plane.

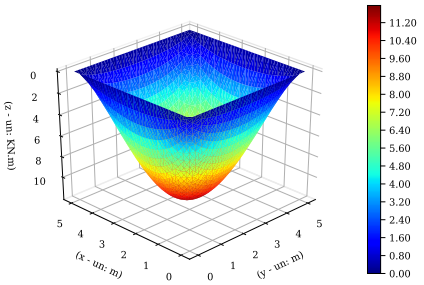


Figure 25 - Bending moment about the ***y-axis*** (M_y) - 3D view in the ***xyz plane.***

Problem 3 – Square plate with three simply supported sides and one clamped side

The following problem involves a square plate with one clamped edge and three simply supported edges under uniformly distributed loading, as shown in Figure 26.

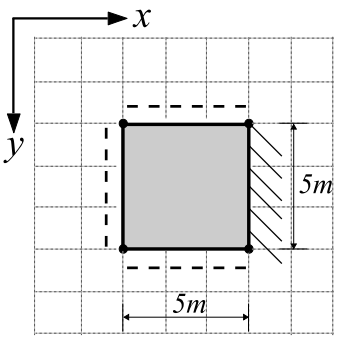


Figure 26 – Square plate with three supported edges and one clamped edge.

The assumptions listed in Table 9 were adopted.

The following table shows the results obtained for Problem 3:

In turn, Figures 27 through 32 represent the displacements and stress in the plate under study.

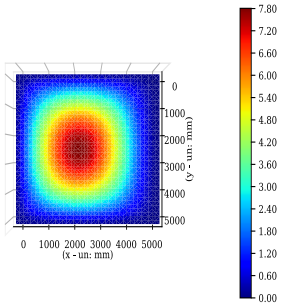


Figure 27 - Displacements (w) - View of the ***xy*** plane.

DOI https://doi.org/10.22533/at.ed.13176226240211

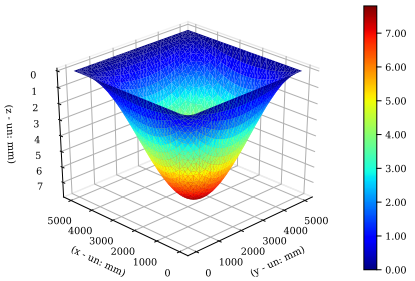


Figure 28 - Displacements (w) - 3D ***xyz*** view.

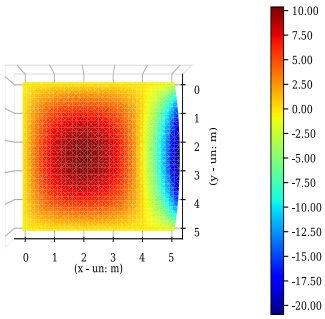


Figure 29 - Bending moment on ***the x-axis*** (M_x) - View in the ***xy*** plane.

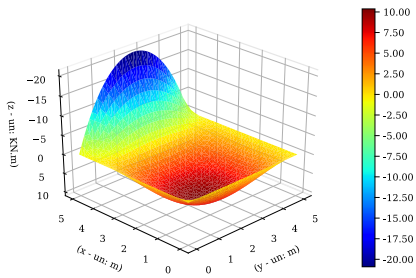


Figure 30 - Bending moment ***about the x-axis*** (M_x) - 3D ***xyz*** view.

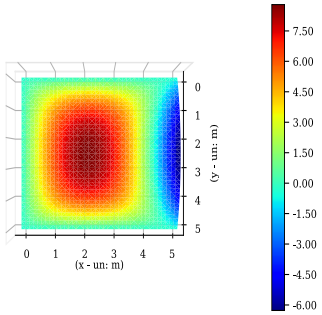


Figure 31 - Bending moment about ***the y-axis*** (M_y) – View in the ***xy*** plane.

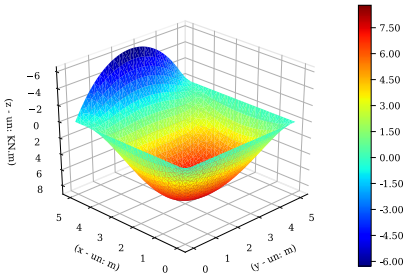


Figure 32 - Bending moment ***about the y-axis*** (M_y) - 3D ***xyz*** view.

Problem 4 – Square plate with two simply supported sides and two fixed sides

The following problem involves a square plate with two clamped edges and two simply supported edges under uniformly distributed loading.

DOI https://doi.org/10.22533/at.ed.13176226240211

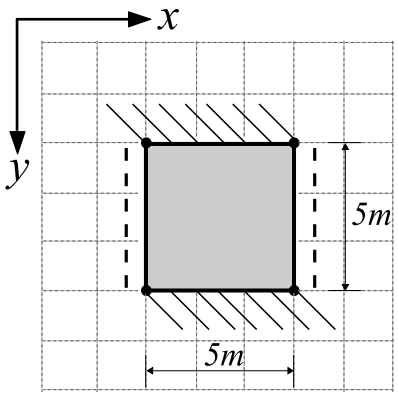


Figure 33 – Square plate with two supported edges and two clamped edges.

The initial assumptions adopted are shown in Table 11.

The following table summarizes the results obtained for Problem 4:

The elapsed time was 12 minutes and 47 seconds. In this example, the errors can be considered satisfactory. As in the second example presented, the error and time values are acceptable and relatively similar, allowing us to conclude that this example was successful. Finally, Figures 34 through 39 represent the displacements and stress in the plate under study.

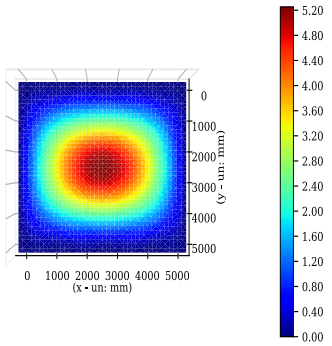


Figure 34 - Displacements (w) - View of the ***xy*** plane.

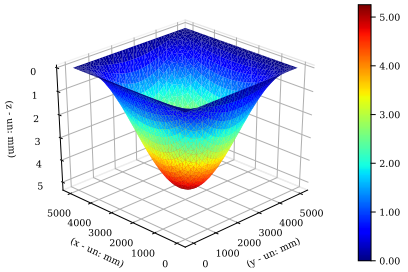


Figure 35 - Displacements (w) - 3D ***xyz*** view.

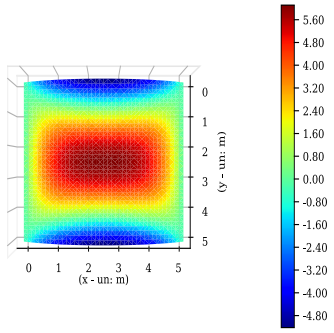


Figure 36 - Bending moment on the ***x-axis*** (M_x) - View of the ***xy*** plane.

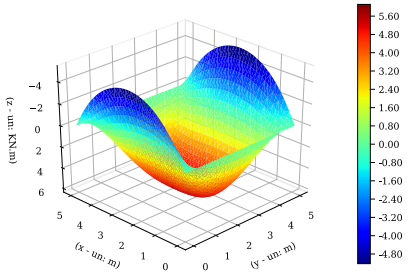


Figure 37 - Bending moment about the x-axis (Mx) - 3D xyz view.

DOI https://doi.org/10.22533/at.ed.13176226240211

q	L	C	E	esp	υ	h
10 kN/m	5 m	5 m	$25x10^6$ kPa	10 cm	0.3	0.125 m
$D = \frac{Eesp^3}{12(1-\upsilon^2)} = 2289{,}3773\ KN.m$						

Table 11 – Initial assumptions adopted.

Results	$w_{máx}$ (mm)	$M_{xmáx}$ (kN·m)	$M_{ymáx}$ (kN·m)
Algorithm	5.254	6.113	-17.412
Analytical[1]	5,242	6,100	-17,425
Error (%)	0.54	0.21	0.075

Table 12—Results obtained.

q	L	C	E	esp	υ	h
10 kN/m	4 m	8 m	$25x10^6$ kPa	10 cm	0.3	0.125 m
$D = \frac{Eesp^3}{12(1-\upsilon^2)} = 2289{,}3773\ KN.m$						

Table 13 - Initial assumptions

Results	$w_{máx}$ (mm)	$M_{xmáx}$ (kN·m)	$M_{ymáx}$ (kN·m)
Algorithm	11.330	7.453	16.265
Analytical[2]	11,327	7,424	16,272
Error (%)	0.03	0.39	0.04

Table 14—Results obtained.

1. The analytical solution is obtained from Table 4 for the ratio $b/a = 1$.
2. The analytical solution is obtained from Table 2 for the ratio $b/a = 2$, where $a < b$, $a = 4$ m.

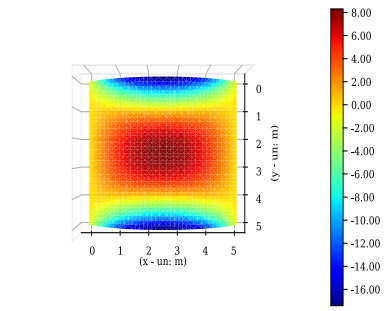


Figure 38 - Bending moment about the y-axis (My) - View in the xy plane.

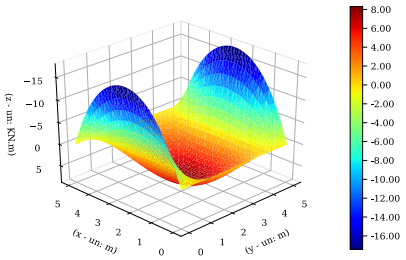


Figure 39 - Bending moment about the y-axis (My) - 3D xyz view.

Problem 5 – Simply supported rectangular plate

The following problem involves a fully supported rectangular plate with uniformly distributed loading.

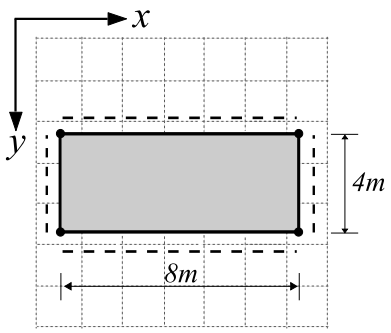


Figure 40 – Rectangular plate with fully supported edges.

The initial assumptions adopted are shown below:

The results obtained for Problem 5 are presented in the following table:

The elapsed time was 23 minutes and 4 seconds. In this example, the errors are considered satisfactory; however, the long processing time compared to the previous examples is due to the geometric shape of the analyzed plate, which has 2048 nodes. Figures 41, 42, 43, 44, 45, and 46 graphically present the results for the displacements and stresses in the plate.

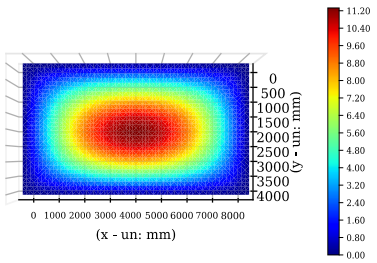


Figure 41 - Displacements (w) - View of the ***xy*** plane.

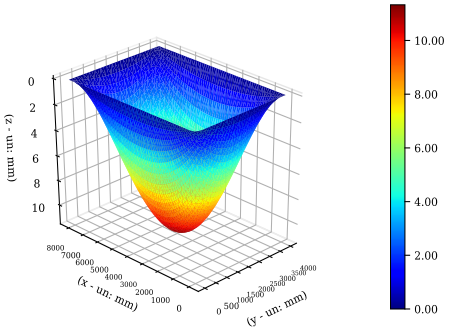


Figure 42 - Displacements (w) - 3D xyz view.

DOI https://doi.org/10.22533/at.ed.13176226240211

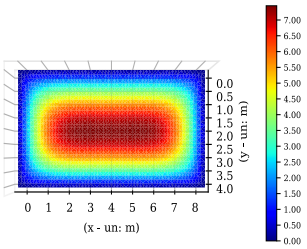


Figure 43 - Bending moment about the x-axis (Mx) - View in the xy plane.

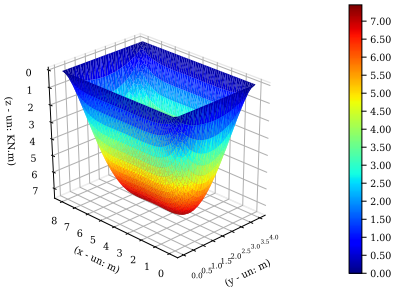


Figure 44 - Bending moment about the x-axis (Mx) - 3D xyz view.

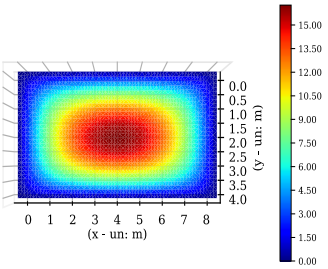


Figure 45 - Bending moment about the y-axis (My) – View in the xy plane.

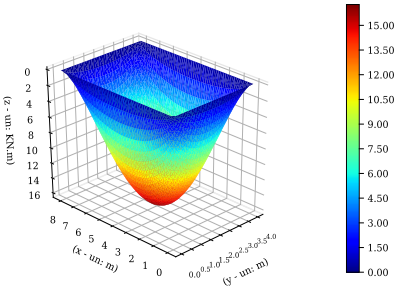


Figure 46 - Bending moment about the y-axis (My) - 3D xyz view.

Problem 6 – Fully clamped *L-shaped* plate

The following problem involves a fully clamped *L-shaped* plate with uniformly distributed loading. Only the deflection was analyzed.

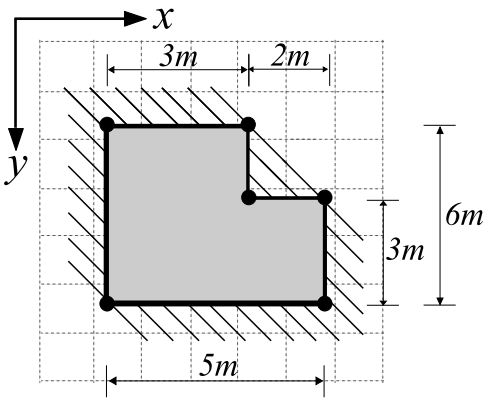


Figure 47 – L-shaped plate with fully fixed edges.

The following are the initial assumptions adopted.

The following table shows the results obtained for Problem 6:

The elapsed time was 9 minutes and 23 seconds. This example differs significantly in terms of the plate's geometry, which led to the results being compared with

q	L	C	E	esp	υ	h
30 kN/m	5 m	6 m	$28x10^6$ kPa	20 cm	0.3	0.125 m
$D = \frac{Eesp^3}{12(1-\upsilon^2)} = 20512{,}82051\ KN.m$						

Table 15 – Initial assumptions adopted.

Results	(mm)
Algorithm	6.814
FEMAP with NX Nastran[1]	6.877
Error (%)	0.92

Table 16—Results obtained.

q	L	C	E	esp	υ	h
13,435 lb	12 in	12 in	$10.3x10^6$psi	0.127 in	0.3	0.375 in
$D = \frac{Eesp^3}{12(1-\upsilon^2)} = 1932{,}082866\ lb.in$						

Table 17 – Initial assumptions adopted.

Results	$w_{máx}$ (in)	Error relative to the algorithm (%)
Algorithm	0.362	
Reference[2]	0.375	3.47
Femap with NX Nastran[3]	0.362	0

Table 16 - Results obtained

1
2
3

DOI https://doi.org/10.22533/at.ed.13176226240211

those of a well-known software package. The error can be considered acceptable, as can the elapsed time. Furthermore, Figures 48, 49, and 50 highlight the displacements in the plate under study.

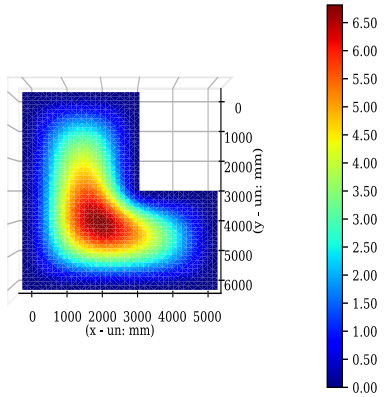


Figure 48 - Displacements (w) - View in the xy plane.

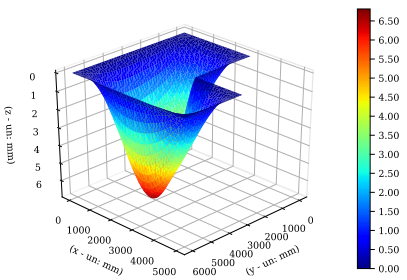


Figure 49 - Displacements (w) - 3D view (A) xyz.

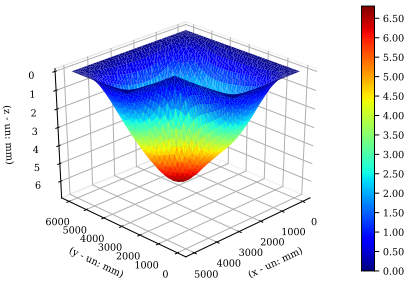


Figure 50 - Displacements (w) - 3D view (B) xyz.

Problem 7 – Square plate with a point load, one fixed side, and three free sides

The following problem involves a square plate with one fixed edge and three free edges, with a point load on the y-axis of symmetry and at the x-end.

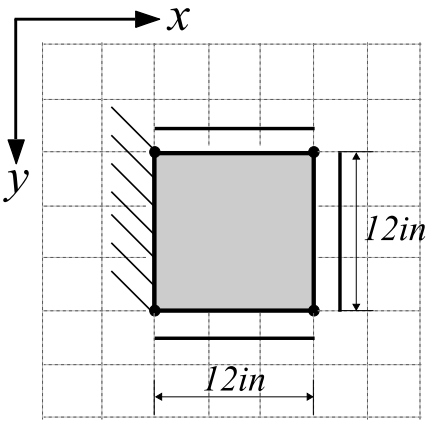


Figure 51 – Square plate with a point load, one fixed edge, and three free edges.

The initial assumptions adopted are presented in the following table.

The results obtained for Problem 7 are shown below:

The elapsed time was 1 minute and 55 seconds. This example requires greater attention due to the free edges. The displacements for two different step values *h* are shown below. The displacements of the plate are shown in Figures 52, 53, 54, and 55.

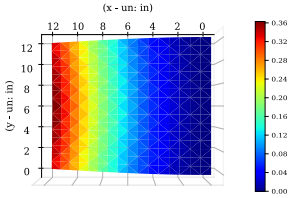


Figure 52 - Displacements (w) (h = 0.75 in) - ***xy*** plane view.

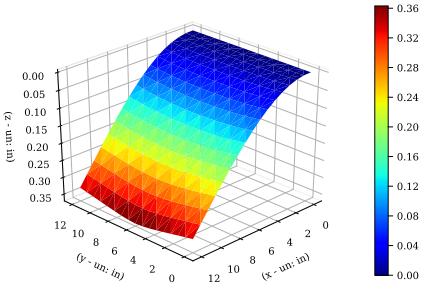


Figure 53 - Displacements (w) (h = 0.75 in) - 3D xyz view.

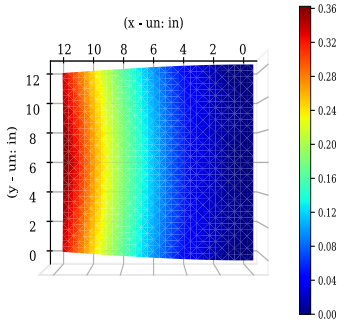


Figure 54 - Displacements (w) (h = 0.375 in) - View of the xy plane.

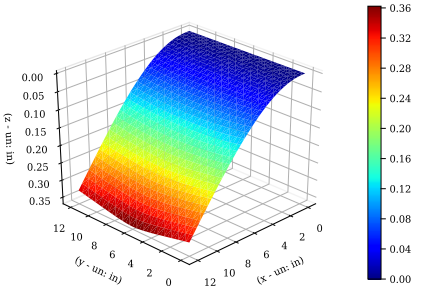


Figure 55 - Displacements (w) (h = 0.375 in) - 3D ***xyz*** view.

CONCLUSION

This work has allowed for the consolidation of theoretical and computational knowledge related to numerical structural analysis, with an emphasis on the application of the Finite Element Method (FEM). The implementation of the matrix formulation of stiffness for truss structures enabled not only a deeper understanding of the mathematical fundamentals involved—equilibrium, compatibility, and constitutive relations—but also the translation of these concepts into a functional computational tool.

The results obtained demonstrated that the developed algorithm was capable of reproducing, with good accuracy, the expected nodal displacements, showing discrepancies within an acceptable range when compared to examples from the literature and established structural analysis software. Such consistency validates both the adopted formulation and the strategy for assembling the global stiffness matrix and applying boundary conditions.

From a computational standpoint, the implementation allowed for a deeper mastery of the programming language used, exploring libraries focused on matrix manipulation, solving linear systems, and algorithmic organization. The development of the routine highlighted the importance of the code's logical structure, the organization of degrees of freedom, and efficiency in the process of assembling global matrices.

In addition to technical validation, the work makes a significant educational contribution, since the actual construction of the algorithm provides a more robust understanding of the internal workings of the FEM, in contrast to the exclusive use of commercial software. The integration of geometric modeling and numerical structural analysis reinforces the practical applicability of the proposed methodology.

Overall, it is concluded that the main objective—to develop and validate an algorithm for linear structural analysis—was fully achieved, establishing a solid foundation for future extensions involving greater geometric complexity, numerical refinement, or nonlinear analyses.

REFERENCES

BARTON, M. V. **Finite Difference Equations for the Analysis of Thin Retangular Plates with Combinations of Fixed and Free Edges**. University of Texas, Defense Research Lab., Austin, 1948.

BEER, Ferdinand P.; E. JOHNSTON, R. Jr., DEWOLF, J. T.; MAZUREK, D. F. **Mecânica dos Materiais**. 5 ed. McGraw-Hill, 2011.

GHALI, A.; NEVILLE, A. M.; BROWN, T. G. **Structural Analysis: A Unified Classical and Matrix Approach**. 6 ed. CRC Press Taylor - Francis Group, 2009.

GILAT, A.; SUBRAMANIAM, V. **Métodos numéricos para engenheiros e cientistas: Uma introdução com aplicações usando o MATLAB**, Bookman, Porto Alegre, 2008.

HIBBELER, R. C. **Resistência dos Materiais**. 7 ed. Pearson, 2010.

JÚNIOR, S. D. C. **Elaboração de um Programa Computacional para o Cálculo e Dimensionamento de Lajes Maciças**. 2008. 105 páginas. Trabalho de Conclusão do Curso Graduação em Engenharia Civil - Universidade Federal de Juiz de Fora, 2008.

MOIN, P. (2010). **Fundamentals of Engineering Numerical Analysis.** Cambridge: Cambridge University Press.

SZILARD, R. **Theories and Applications of Plate Analysis: Classical, Numerical, and Engineering Methods.** 2nd ed. John Wiley & Sons, 2004.

TIMOSHENKO, S.; WOINOWSKY-KRIEGER, S. **Theory of Plates and Shells.** 2nd ed. McGraw-Hill, 1959.

UGURAL, Ansel C. **Stresses in Beams, Plates, and Shells**. CRC Series in Computational Mechanics and Applied Analysis. 3rd ed. CRC Press Taylor & Francis Group, 2009.